# Strathprints Institutional Repository

**Alshammary, Abdullah and Weiss, Stephan and Soraghan, John and Almorqi, Sultan (2014) Wideband 2-Dimensional scanning planar subarray. In: 10th IMA International Conference on Mathematics in Signal Processing. Institute of Mathematics and its Applications. ,**

This version is available at http://strathprints.strath.ac.uk/57852/

# Wideband 2-Dimensional scanning planar subarray

Abdullah Alshammary[*], Stephan Weiss[*], John Soraghan[*], and Sultan Almorqi[**]

[*]EEE Department, University of Strathclyde, Glasgow, UK
[**]KACST, Riyadh, Saudi Arabia

*Abstract*—**Achieving frequency invariance in antenna array requires linear-phase system to maintain frequency independent time lag. For example True Time Delay or tapped delay line. In this paper, the array elements are divided into subarrays. Then all subarrays are steered towards the desired azimuth direction, while the wideband property is preserved by exploiting the subarray two-dimensional structure as a sensor delay line. Each subarray pattern is then individually rotated around the desired elevation direction. Eventually superposition of subarrays is maximally constructive towards the desired direction and partially constructive or destructive everywhere else. Two frequency invariant beamformers are used. These are inverse DFT and Least squares. Results are compared with wideband wideband one-dimensional pattern syntheses of the same design methods in power concentration.**

*Keywords*: sensor delay line, wideband beamforming, subarray

## I. INTRODUCTION

Sensor delay line is one of the most flexible approaches to antenna array spatial and frequency coverage. A planar array can be narrowband with two dimensional pattern control or wideband one dimensional pattern. The versatility of sensor delay line allow changing the response bandwidth and pattern without changing the antenna architecture. In applications where the signal of interest is broadband and elevation angle is fixed, the sensors parallel to incidence direction can sample the signal in time with a delay proportional to $\sin\theta$. This function is similar to that of the tapped delay line only with no dependency on angle $\theta$.
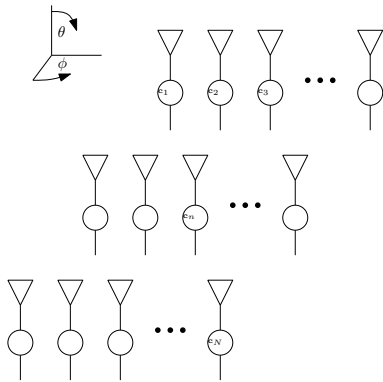


Fig. 1. Planar array model consisting of elements distributed evenly on x and y axis. Each element have an attached weight.

However the full sacrifice of elevation angle for the sake bandwidth can be avoided by introducing a compromise between the two through subarray structure. If the array is divided into smaller groups, each subarray can be given a wideband pattern. When superimposed together the overall response will have the common features of the individual subarrays.

## II. ARRAY ANALYSIS

the time spent for a signal to travel to any point in the antenna structure compared to the reference point is

$$\tau = \frac{\mathbf{kr}}{\omega}$$

$$\text{where} \quad \mathbf{k} = \frac{\omega}{c} \begin{bmatrix} \sin\theta\cos\phi \\ \sin\theta\sin\phi \\ \cos\theta \end{bmatrix} \tag{1}$$

$$\tag{2}$$

Where $\omega$ is the angular frequency. $\theta$ and $\phi$ are the elevation and azimuth angles respectively. The $\mathbf{kr}$ represents the projection of sensor location vector $\mathbf{r}$ onto the propagation unit vector $\mathbf{k}$. When divided by speed of sound, $c$ the projection indicate time delay $\tau$. Notice that any element distribution can be represented in equation (1). the The radiation pattern of an antenna is the resultant of the current excitation $I(\mathbf{r})$ as follows:

$$H(\omega, \theta, \phi) = \int_{r \in R} I(\mathbf{r}) e^{-i\omega\tau} dr \tag{3}$$

Where $R$ is the set of elements locations. For antenna array with discrete number of identical elements $N$ with frequency and angle response $D(\omega, \theta, \phi)$. The array pattern is the sum of products of the element steering vector elements weights. The above equation the reduces to its discrete form.

$$H(\omega, \theta, \phi) = \sum_{n=1}^{N} D(\omega, \theta, \phi) \mathbf{c}_n e^{-i\omega\tau_{\mathbf{n}}} \tag{4}$$

$\mathbf{c}_n$ is the weighting attached each antenna element with index $n$. The following analysis will assume isotropic elements hence $D$ is omitted.Alternatively for non-isotropic elements the resultant weighting should divided by the element response. $\hat{\mathbf{c}}_n = \frac{\mathbf{c}_n}{D}$ where $\hat{\mathbf{c}}_n$ is the effective weighting to be applied to the element of index $n$. To use vector format then the steering vector need to be defined as the set of lag experience with respect to zero lag $\tau_{\dot{n}}$ corresponding to the

reference point $\mathbf{r}_{\dot{n}}$.

$$\mathbf{s} = \begin{bmatrix} e^{-i\omega\tau_1} \\ \dots \\ e^{-i\omega\tau_{\dot{n}}} \\ \dots \\ e^{-i\omega\tau_N} \end{bmatrix} \tag{5}$$

The vector form of array response then becomes

$$H = \begin{cases} \mathbf{c}^T S & \text{if } D = 1 \\ \hat{\mathbf{c}}^T S & \text{otherwise} \end{cases} \tag{6}$$

*1) Inverse Discrete Fourier Transform:* two dimensional Inverse Discrete Fourier Transform IDFT has been used with rectangular, uniform spacing array to synthesis wideband beamformer. For planar array, if sensor location $r$ is distributed evenly on $x$ and $y$ with spacings $d_x$ and $d_y$. For IDFT case, the element indexing will be separated to the $x$ and $y$ axis to $n$ and $m$ respectively. Not to be confused with previous $n$ index. The radiation pattern now reduces to

$$H = \sum_{n=-\frac{N}{2}}^{\frac{N}{2}} \sum_{m=-\frac{M}{2}}^{\frac{M}{2}} \mathbf{c}_{nm} e^{-i\frac{\omega}{c}\sin\theta(nd_x\cos\phi+md_y\sin\phi)} \tag{7}$$

Where $d_x$ and $d_y$ are x and y elements spacings respectively and $\mathbf{c}_{nm}$ is the weight attached to the element located at $[nd_x, md_y, 0]^T$ . From the above equation , two spatio-temporal variables $\omega_x$ and $\omega_y$ can be defined as follows

$$\omega_x = \frac{\omega}{c} d_x \sin\theta\cos\phi$$
$$\omega_y = \frac{\omega}{c} d_y \sin\theta\sin\phi \tag{8}$$

Hence the radiation pattern in terms of newly defined frequencies is.

$$H(\omega_x, \omega_y) = \sum_{n=-\frac{N}{2}}^{\frac{N}{2}} \sum_{m=-\frac{M}{2}}^{\frac{M}{2}} \mathbf{c}_{nm} e^{-i(n\omega_x+m\omega_y)} \tag{9}$$

Equations (9) above fits the definition of tow dimensional Discrete Fourier transform. It is often desirable to obtain an array response over the frequency band of interest to imitate a specific pattern, say the desired waveform $P_d(\omega, \theta, \phi)$. Desired pattern is real if array weights are real and can be complex valued if weights are complex. To obtain the required weights for a given desired response, the inverse transformation is applied:

$$\mathbf{c}_{nm} = \sum_{\omega_x=-\pi}^{\pi} \sum_{\omega_y=-\pi}^{\pi} P_d(\omega_x, \omega_y) e^{i(n\omega_x+m\omega_y)} \tag{10}$$

Notice that similarity with circular symmetric weighting in [8, p. 259]. Comparing equation (10) with two dimensional DFT approach in [2], [3], [6] reveal that the former is more general and applicable to non uniform and arbitrary shape.

*2) Least Squares:* Recalll from equation 6 that the array response can be represented in vector format as the product of weights and the steering vector as follows.

$$H = \mathbf{c}^T \mathbf{s}(\omega, \theta, \phi) \tag{11}$$

The error quantity can be defined as the squared deviation of the desired pattern $P_d$ from the array response $H$.

$$e = P_d(\omega, \theta, \phi) - H(\omega, \theta, \phi) = P_d - \mathbf{c}^T \mathbf{s}$$

Least square approach minimizes the squared error. Complex matrices are spared by multiplying the matrix buy it is conjugate transpose. Hence the squared error (SE) becomes:

$$SE = [P_d - \mathbf{c}^T\mathbf{s}][P_d - \mathbf{c}^T\mathbf{s}]^H$$
$$= (P_d - \mathbf{c}^T\mathbf{s})(P_d^H - \mathbf{s}^H\mathbf{c}^*)$$
$$= P_d^2 - 2\mathbf{c}^T P_d\mathbf{s} + \mathbf{c}^T(\mathbf{s}\mathbf{s}^H)\mathbf{c}$$

The term $P_d \mathbf{s}$ is the correlation vector $\mathbf{d}$ and the $\mathbf{s}\mathbf{s}^H$ is the covariance matrix $R$. This error is calculated at specific frequency and angle. To obtain the mean error over the operating frequency and space, $SE$ is integrated over the frequency and angles.

$$MSE = \int_\omega \int_\theta \int_\phi P_d^2 - 2\mathbf{c}^T\mathbf{d} + \mathbf{c}^T R\mathbf{c}$$
$$= 1 - 2\mathbf{c}^T\hat{\mathbf{d}} + \mathbf{c}^T \hat{R}\mathbf{c}$$

apparently squared error is a quadratic function of $\mathbf{c}$. The least point can be found by differentiating w.r.t $\mathbf{c}$ then finding the null space of the result [8].

$$\frac{\partial}{\partial\mathbf{c}^T} 1 - 2\mathbf{c}^T\hat{d} + \mathbf{c}^T \hat{R}\mathbf{c}$$
$$= 0 - \hat{\mathbf{d}} - 0 - \hat{R}\mathbf{c}$$

Hence the set of weights that achieves the least squared error is

$$\mathbf{c} = \hat{R}^{-1}\hat{\mathbf{d}} \tag{12}$$

where $\hat{R}$ is the integration of the square $N\mathrm{x}N$ covariance matrix over space and frequency. $\mathbf{d}$ is $N\mathrm{x}1$ column vector as follows:

$$\hat{R} = \int_\omega \int_\theta \int_\phi R(\omega, \theta, \phi)\, d\omega d\theta d\phi$$
$$\hat{\mathbf{d}} = \int_\omega \int_\theta \int_\phi P_d\mathbf{s}(\omega, \theta, \phi)\, d\omega d\theta d\phi \tag{13}$$

## III. EFFECT OF ASSUMING FIXED ELEVATION ANGLE

Many analysis of 2-dimensional array using sensor delay line assumed fixed elevation angle [5], [1]. Most have chosen 90 degrees elevation which corresponds to incident or transmitted waves parallel to the array geometric plane. Such assumption is valid for wideband signal if the beamformer response to any other elevation direction is irrelevant. Elevation angle has the same effect to that steering vector as the signal frequency. To illustrate that lets reconsider equation (7).

Notice that the term $\frac{\omega}{c}\sin\theta$ is dependent on both frequency and elevation angle. When defining any desired pattern it is not possible to discriminate between frequency and elevation angle. both parameters can vary according to the following relationship and still produce the same array response.

$$\frac{\omega}{c}\sin\theta = constant \qquad (14)$$

Near broadside direction the response is less sensitive to angle. This is desirable area for wider frequency band.

## IV. ROTATED ELEVATION CONSTRAINT

The phase of array response in (4) depend on both frequency and elevation angle. When defining any desired pattern it is not possible to discriminate between frequency and elevation angle. Both parameters can vary according to the following relationship and still produce the same array response. To resolve the elevation angle ambiguity, Subarrays can be steered to the desired azimuth angle, and then individually rotated around the desired elevation angle. Recall equation (10) used to calculate array weights. Azimuth angle $\phi$ instead of being constant can be a function of the elevation angle.

$$\hat{\phi_m} = \phi - \alpha_m(\theta - \theta_0) \qquad (15)$$
$$\text{where} \qquad m = 0, \ldots, M$$

the effect $\hat{\phi_m}$ has on the pattern is to twist the pattern as elevation angle changes. However, at the desired elevation angle $(\theta - \theta_0)$ the subarrays align with others. In order to minimize the total array response in the sidelobe region, the pattern should be symmetric around $\phi_0$. When this balance is maintained the subarrays cancels each other as long as the beamwidth is smaller than $\hat{\phi} - \phi_0$. twist is inflected on the wavenumber vector $\mathbf{k}$ and its components $u$ and $v$ it will then be as follows.

$$\frac{c}{\omega}\mathbf{k}(\theta, \hat{\phi_m}) = \begin{bmatrix} \hat{u} \\ \hat{v} \end{bmatrix} = \begin{bmatrix} \sin\theta\cos\hat{\phi} \\ \sin\theta\sin\hat{\phi} \end{bmatrix} \qquad (16)$$

To illustrate the effect on the steering matrix lets substitute equation (15) in(16)

$$\mathbf{k}(\theta, \phi_m) = \begin{bmatrix} \sin\theta\cos\phi\sin\beta + \sin\theta\sin\phi\sin\beta \\ \sin\theta\sin\phi\sin\beta + \sin\theta\cos\phi\sin\beta \end{bmatrix} \qquad (17)$$
$$\text{where } \beta = \alpha(\theta - \theta_0)$$

Here, $\beta$ represents the product of subarray slope $\alpha$ and elevation deviation.

$$\mathbf{k}(\theta, \hat{\phi_m}) = \begin{bmatrix} u\cos\beta + v\sin\beta \\ u\sin\beta + v\cos\beta \end{bmatrix} \qquad (18)$$

Hence the transformation matrix from the rotated elevation wavenumber to array wavenumber is

$$\begin{bmatrix} \hat{u} \\ \hat{v} \end{bmatrix} = \begin{bmatrix} \cos\beta & \sin\beta \\ \sin\beta & \cos\beta \end{bmatrix} \qquad (19)$$

Equation (19) indicates that as the angle $\alpha$ increases, $\hat{u}$ moves away u. Hence, the $uv$ coordinates rotates with angle $\alpha$.
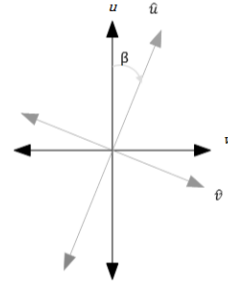


Fig. 2. Desired pattern of least square approach at center frequency $0.66\pi$

In rotated elevation constraint approach, the constraint is applied to the elevation angle $\theta$. Recall from equation (1) that $\sin\theta$ is common term in both $u$ and $v$. An incident signal from elevation angle $\theta_1$ and frequency $f_1$ can produce the same response as another signal from elevation angle $\theta_2$ a and $f_2$ given that they satisfy the following equation:

$$\frac{f_1}{f_2} = \frac{\sin\theta_2}{\sin\theta_1} \qquad (20)$$

Resulting in beam squint that relates to frequency deviation as

$$\theta = \sin^{-1}(\sin\theta_0 \frac{f_0}{f}) \qquad (21)$$

## V. POWER CONCENTRATION MEASUREMENTS

Array ability to concentrate power in the desired direction is introduced in [4] as the ratio between power concentration to the total dissipated power into the upper far field hemisphere. The power dissipated over

$$\psi(\omega, \theta, \phi) = \int_\omega \int_\theta \int_\phi |H(\omega, \theta, \phi)|^2 d\omega d\theta d\phi \qquad (22)$$

The concentrate power can be rewritten as follows.

$$\rho(\omega, \theta, \phi) = \frac{\psi(\omega, \theta, \phi)}{\int_{-\pi/2}^{\pi/2}\int_{-\pi}^{\pi}\psi(\omega, \theta, \phi)d\theta d\phi} \qquad (23)$$

Substituting $\psi$ in equation (7) results in

$$\psi(\omega, \theta, \phi) = \frac{\mathbf{c}^T \hat{R}\mathbf{c}}{\mathbf{c}^T\mathbf{c}} \qquad (24)$$

Where $\hat{R}$ is the average sensor covariance matrix calculated from (13).

## VI. SIMULATIONS AND RESULTS

Concentrated power measurements in this example it is a cone with $15°$ radius around the reference angle. The wide cone is required to compensate for squinting effect over frequency which is noticeable in rotated elevation. Power concentration is presented here for the array excitations are calculated using IDFT and least squares approaches. Results are compared to conventional 1-D wideband sensor delay line approach described in [2], [3], [7], [1]. In 1-D case the planar array is used as one dimensional array treated without division to subarrays. While the other dimension is used for temporal filtering. All elements are used in the synthesis of

one-dimensional azimuth pattern. The elevation is fixed at the desired elevation angle of $35°$. The array is constructed by 3x3 hexagonal subarrays containing 44 elements each. The look angle is $0°$ azimuth and $35°$ elevation. The desired response is a Taylor window with -90 sildeobe level. Rotation slope between azimuth and elevation varies between -1.5 and 1.5.
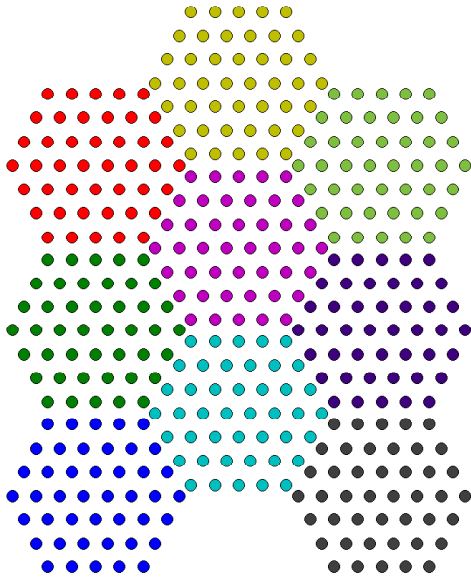


Fig. 3. 3x3 hexagonal subarray used for simulation. Element spacing is 30 cm corresponding to $\frac{\lambda}{2}$

### A. 2-D Invers Descrete Fourier Transform

Individual subarrays pattern is shown below. Each subarray is steered individually by its unique slope. Notice how all subarrays illuminate the desired direction but have different response elsewhere.
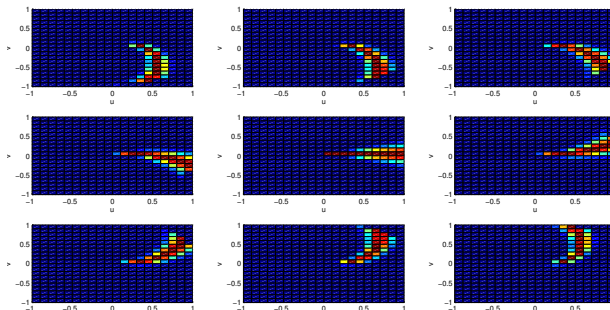


Fig. 4. Individual subarray pattern for the 3x3 array being simulated in $uv$ coordinated described above.

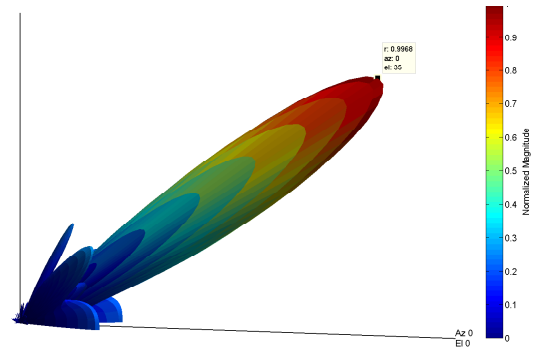IDFT method produced the cleanest mainlobe and relatively low grating lobes over the frequency band.



Fig. 5. 3D normalized magnitude pattern of rotated elevation constraint using IDFT method

rotated elevation method show relatively flat gain over frequency band compared to conventional 1-D approach. This means that grating lobes are small or are from the look direction since they cause sudden change in gain over frequency.
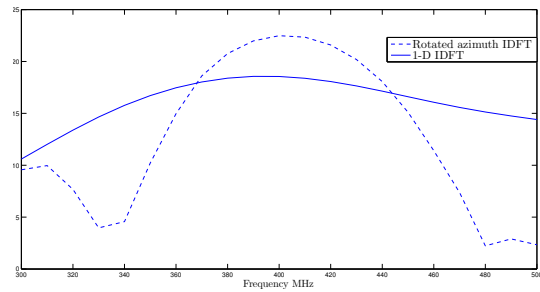


Fig. 6. Power concentration comparison between conventional 1-D pattern IDFT synthesis and one using proposed rotated elevation constraint method

### B. Least squares

Grating lobes are close in magnitude to the main lobe. Grating lobes numbers and locations vary with frequency and their effect can be seen in the gain graph.
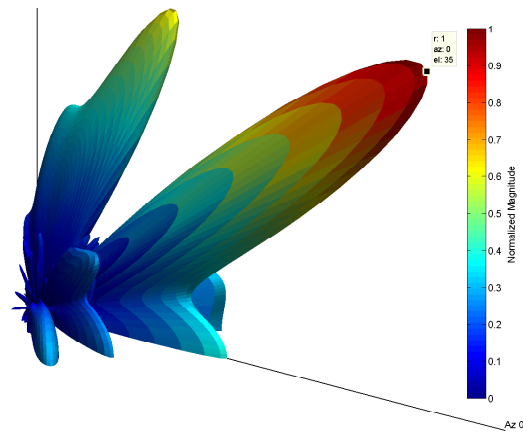


Fig. 7. 3D pattern at 400 MHz center frequency obtained by the proposed rotated elevation constraint method using least squares approach

When grating lobe move into the look angle cone around 330 MHz the power concentration increases drastically.
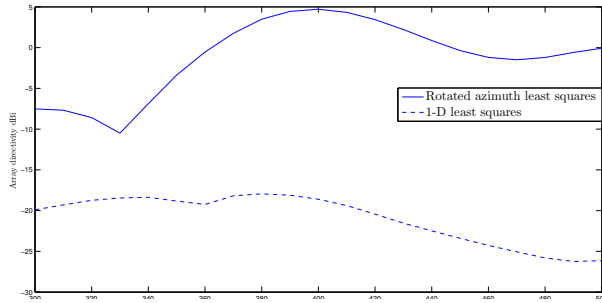
Fig. 8. Concentrated power comparison between conventional 1-D pattern synthesis and the proposed rotated elevation constraint method using least squares approach

## VII. Conclusion

Rotated elevation method provides a compromise for planar arrays between narrowband 2-dimensional space steering and wideband sensor delay line with 1-dimensional steering in azimuth only. This is achieved by dividing the array into subarrays and steer them toward the desired azimuth angle. Then individually rotate each subaarry using a unique slope around the desired elevation angle. Results indicate acceptable gain flatness and power concentration but introduced high grating lobes close to the look direction. Superposition of multiple 1-D smaller arrays caused movement of grating lobes around the mainlobe.

## References

[1] A. Alshammary. Frequency invariant beamforming using sensor delay line. In *Electronics, Communications and Photonics Conference (SIECPC), 2011 Saudi International*, pages 1–5, 2011.

[2] M. E. Bialkowski and M. Uthansakul. A wideband array antenna with beam-steering capability using real valued weights. *Microwave and Optical Technology Letters*, 48(2):287–291, 2006.

[3] M. Ghavami. Wideband beamforming using rectangular arrays without phase shifting. *European Transactions on Telecommunications*, 14(5):449–456, 2003.

[4] P. Karagiannakis, S. Weiss, G. Punzo, M. Macdonald, J. Bowman, and R. Stewart. Impact of a purina fractal array geometry on beamforming performance and complexity.

[5] W. Liu. Adaptive wideband beamforming with sensor delay-lines. *Signal Processing*, 89(5):876 – 882, 2009.

[6] W. Liu and S. Weiss. *Wideband Beamforming: Concepts and Techniques*. Wireless Communications and Mobile Computing. Wiley, 2010.

[7] M. Uthansakul and M. Bialkowski. Fully spatial wide-band beamforming using a rectangular array of planar monopoles. *Antennas and Propagation, IEEE Transactions on*, 54(2):527–533, 2006.

[8] H. L. Van Trees. *Optimum Array Processing (Detection, Estimation, and Modulation Theory, Part IV)*. Wiley-Interscience, 1 edition, Mar. 2002.